

# The Use of Semi-Adiabatic Calorimetry for Hydration Studies of Cement Paste

Chung, Chul-Woo      Kim, Ji-Hyun      Lee, Soo-Yong\*

*Department of Architectural Engineering, Pukyong National University, Nam-gu, Busan, 48513, Republic of Korea*

---

## Abstract

The semi-adiabatic calorimetry technique is a robust and easy technique that can be used to measure the temperature rise of concrete. This method is often used for investigating the maturity of concrete, as well as to predict maximum temperature rise of mass concrete using various heat loss compensating models. Semi-adiabatic calorimetry can also be used for predicting setting time of concrete. However, it has seldom been used to investigate the hydration characteristics of various cement paste samples. In this research, semi-adiabatic calorimetry and X-ray diffraction methods were used to investigate the hydration characteristics of 3 different ASTM type I Portland cements. First derivative of temperature rise ( $dT/dt$ ) curve was used to isolate individual peaks. Based on the results of the experiments, a combination of  $dT/dt$  curve with XRD could be used to successfully identify hydration at a specific time period, showing its potential to be used as an alternative tool for hydration studies of cement-based materials.

Keywords : semi-adiabatic, calorimetry, hydration, cement paste

---

## 1. Introduction

Calorimetry is the measurement of heat from chemical reactions or physical changes [1]. For cement and concrete applications, two types of calorimeter, isothermal and adiabatic calorimeters, have been used. The term “isothermal” indicates that there is no change in the temperature during the experiments. Therefore, isothermal calorimetry uses a very small amount of sample (approximately 15g or less, in most cases 1 to 2 grams of cement paste) to avoid temperature gradient within the sample. With isothermal calorimetry, when cement paste hydrates and generates the heat of hydration, the heat will

flow from the cement paste through the thermopile (or any type of sensor) toward the surrounding isothermal environment; the amount of heat passing through the sensor can be measured using this concept. Therefore, isothermal calorimetry can be effectively used to characterize the heat of hydration associated with any kind of chemical reaction occurring at specific time period [2,3,4].

The term “adiabatic” means that there is no change in the heat flow during an experiment[5]. Adiabatic calorimetry measures temperature changes in a sample by preventing heat flow in or outside of an insulated chamber. The complete insulation of the chamber is almost impossible, so in most cases, a heating circuit and sensor are installed in the chamber to compensate for heat loss through the environment; if this is not possible, alternative numerical modeling methods should be used for prediction of maximum temperature in mass concrete[6]. The condition measured by adiabatic

---

Received : January 18, 2016

Revision received : February 15, 2016

Accepted : February 19, 2016

\* Corresponding author: Lee, Soo-Yong

[Tel: 82-51-629-6089, E-mail: leesy@pknu.ac.kr]

©2016 The Korea Institute of Building Construction, All rights reserved.

calorimetry is very similar to that condition at the center of the mass concrete that does not allow the heat of hydration to be dissipated. In adiabatic calorimetry curve, the temperature keeps rising as hydration continues, and presents a plateau although the rate of hydration has been significantly decreased[7,8]. As a result, the calorimetry data does not present any specific peak, and if it does it is rather smooth or sometimes almost unclear, although the temperature rise of the specimen indicates the heat being produced during the hydration.

The major difference between isothermal and adiabatic calorimetry is in the point at which the adiabatic calorimetry will be able to characterize the effect caused by the acceleration of reaction due to temperature rise associated with hydration. However, in most cases, adiabatic calorimetry has been only used for measuring maximum temperature level to predict the degree of thermal cracking for mass concrete applications.

Recently, a semi-adiabatic calorimetry technique has been used for predicting the setting time of concrete[9,10]. The reason why it is referred to as semi-adiabatic is that although it is very similar to adiabatic calorimetry in terms of insulation, no correction is being made on heat loss through insulator to the surrounding environment. Actually, the condition of the specimen in semi-adiabatic calorimetry is the closest to the condition of real concrete compared to conditions in both isothermal and adiabatic calorimetry. An additional advantage of this system is the ease of making a test setup. The system can be built up simply using Styrofoam, thermocouple, and thermocouple data logger. Due to this advantage, semi-adiabatic calorimetry is more frequently used in the construction field to measure temperature rise, although this method could be utilized for further applications.

The main purpose of this work is to investigate whether semi-adiabatic calorimetry can be used for

the hydration study of cement paste. This section will first provide an understanding of the characteristics of unhydrated cement, in order to correlate it to that of hydrated cement paste, and to correlate specific hydration reaction to semi-adiabatic calorimetry response. Although this approach is not commonly used for hydration studies, it is necessary to explore the use of semi-adiabatic calorimetry for hydration studies of cement paste.

## 2. Experimental procedure

In order to understand the characteristics of the cements used for this experimental study, x-ray diffraction (XRD), equipped with Cu-K $\alpha$  radiation, was used. To facilitate phase analysis of these cements, both salicylic acid/methanol extraction (SAM) and KOH/sugar extraction methods were applied. SAM extraction was used for identification of C<sub>3</sub>A (aluminate), C<sub>4</sub>AF (ferrite), and minor phases such as calcium sulfate and alkali sulfates through removal of C<sub>3</sub>S (alite), C<sub>2</sub>S (belite), and CaO. KOH/sugar extraction was used for identification of  $\alpha$  - and  $\alpha'$  -C<sub>2</sub>S. These extraction techniques were used because the large number of phases, which makes the analysis of Portland cement difficult, also results in substantial peak overlap.

### 2.1 Salicylic acid/methanol extraction

The sample, 5g of cement or clinker, was added to a solution containing 20g of salicylic acid in 300ml methanol, and the mixture was stirred at room temperature for 2 hours. The suspension was vacuum filtered using a Buchner funnel and a filter paper. The residue was washed with methanol and dried in a 60°C vacuum oven until XRD analysis. In addition, for identifying the C<sub>3</sub>A polymorph, the same SAM extracted samples were heated at 500°C for 1 hour to convert all forms of calcium sulfate to insoluble anhydrite.

## 2.2 Potassium hydroxide/sugar extraction

The sample, 9g of cement, was added to a solution containing 30g of KOH and 30g of sugar at 95°C. The suspension was stirred for one minute. Filtering of solution using filter paper is often difficult, so the suspension was allowed to settle for two minutes, then the top solution was poured off, and the remaining suspension was centrifuged. After centrifuging, the top solution was poured off and the residue was vacuum filtered, washed with 100-ml methanol, and stored in a 60°C vacuum oven until XRD analysis.

## 2.3 Semi-adiabatic calorimetry

Semi-adiabatic calorimetry tests were run on the three cement pastes made with ASTM type I Portland cement[11]. The three cements were named Cement 1, Cement 2, and Cement 3, respectively. The semi-adiabatic calorimetry system used in this experiment is shown in Figure 1.

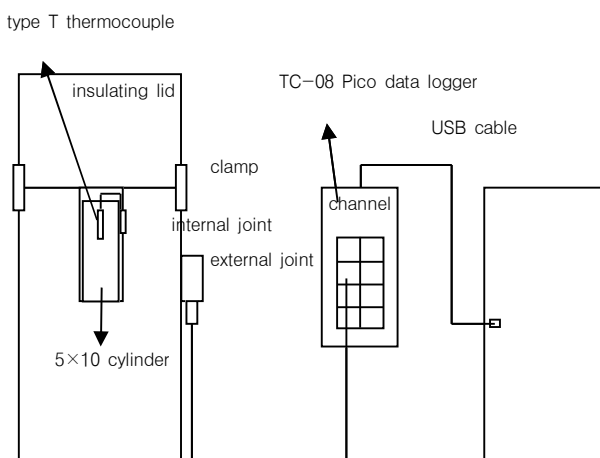


Figure 1. Schematic presentation of semi-adiabatic container for cement paste

The semi-adiabatic calorimetry system consists of Pico Technology data logger TC-08 and its operating software, type T thermocouples, and two heat

insulating containers, which use diameter 5 cm×10 cm cylinders, and is thus a suitable size for cement paste. The container has two connectors: one is for outside connection from data logger to the container, the other is for inside connection from the container to the sample.

All pastes had a water-to-cement ratio of 0.5. Proportion used in the paste was 1500g cement and 750g water. The cement pastes were mixed according to ASTM C 305 procedure[12]. A slight modification was made to prevent splashing of cement paste during mixing.

## 3. Results

### 3.1 Chemical composition of cements

The results are summarized in Table 1. Cement 1 contains high  $C_3A$  and low  $C_4AF$ . The sample contains two types of  $C_3A$ , both the orthorhombic and the cubic form. The sample also contains two types of calcium sulfate, both calcium sulfate hemihydrate ( $CaSO_4 \cdot 0.5H_2O$ ), and gypsum ( $CaSO_4 \cdot 2H_2O$ ). This cement also contains both calcite and periclase. It was also found that tricalcium silicates are present in M1 and M3 form, and most of the dicalcium silicate is in the  $\beta-C_2S$  (larnite) form. Some  $\alpha-C_2S$  is observed, but the relative amount is very small compared to  $\beta-C_2S$ .

Cement 2 also contains two types of  $C_3A$ , cubic and orthorhombic. Unlike Cement 1, this cement contains three types of calcium sulfates, gypsum, hemihydrate, and anhydrite. This cement does not contain any calcite, periclase, or alkali sulfate. Since three types of calcium sulfates are present, stiffening could be an issue. Tricalcium silicates are present in M1 and M3 form, and most of the dicalcium silicate is in the  $\beta-C_2S$  (larnite) form.  $\alpha-C_2S$  was also found.

**Table 1. Summary of XRD phase analysis of three cements**

	Cement 1	Cement 2	Cement 3
C <sub>3</sub> S	Mostly M1, M3 form	Mostly M1, M3	Mostly M1, M3
C <sub>2</sub> S	Mostly β-C <sub>2</sub> S, some α-C <sub>2</sub> S	Mostly β-C <sub>2</sub> S, some α-C <sub>2</sub> S	Mostly β-C <sub>2</sub> S, some α-C <sub>2</sub> S
C <sub>3</sub> A	Orthorhombic and cubic	Orthorhombic and cubic	Orthorhombic and cubic
C <sub>4</sub> AF	Brownmillerite	Brownmillerite	Brownmillerite
Sulfates	Hemihydrate and gypsum	Hemihydrate, gypsum, and anhydrate	Hemihydrate
Other constituents	Calcite, periclase	none	Calcite, periclase

The phase composition of Cement 3 is very similar to that of Cement 1. The sample contains two types of C<sub>3</sub>A, both the orthorhombic and the cubic form. This cement contains both calcite and periclase. However, this cement contains no gypsum, only calcium sulfate hemihydrate (CaSO<sub>4</sub> · 0.5H<sub>2</sub>O). Tricalcium silicates are present, in M1 and M3 form. Most of the dicalcium silicate is in the β -C<sub>2</sub>S (Iarnite) form, but some α -C<sub>2</sub>S was also observed.

**3.2 Semi-adiabatic responses**

The calorimetry curves are presented in Figures 2 and 3. The ranking of cements according to the time to reach maximum temperature was Cement 2 > Cement 1 > Cement 3. The first derivative of temperature rise, presented in Figure 3, indicates that all three cements have more than one hydration peak. Cement 1 has a broad shoulder at about 375 min, a sharp peak at about 460 min, and a broad shoulder at about 520 min. Cement 2 has a shoulder at about 300 min and a sharp peak at about 364 min. Cement 3 has a broad peak at about 480 min and a sharp peak at about 575 min. Based on the calorimetry results, sampling times for XRD analysis were selected, before and after each individual peak observed in Figure 3. The sampling times are listed in Table 2.

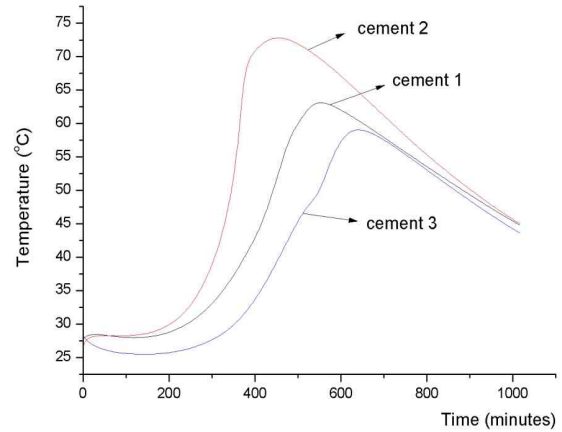


**Figure 2. Semi-adiabatic calorimetry curves for three type I Portland cement pastes**

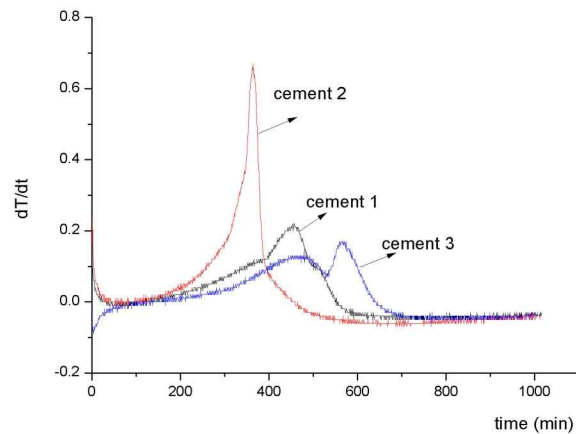


**Figure 3. Semi-adiabatic calorimetry curves for cement pastes showing first derivative with respect to temperature**

**Table 2. Sampling times (min)**

Cement 1	5	160	385	500	580
Cement 2	5	160	348	400	580
Cement 3	5	280	530	720	-

**3.3 Hydrated cement phases**

XRD analyses of hydrated cement pastes were performed on the cements collected at specific times listed in Table 2. After sample was collected from semi-adiabatic container, specimens were placed in a 20-ml glass bottle, filled approximately one-third with paste, and methanol was added to stop hydration. After stopping hydration, sample was analyzed using XRD.

For each cement, XRD patterns were collected on the unhydrated cement, after 5 minutes of hydration and at the sampling times listed in Table 2. The 5-minute sample was taken in order to find evidence of secondary gypsum formation that could be associated with various forms of calcium sulfates in Portland cements. Diffraction angle ( $2\theta$ ) of cement phases for peak intensity measurements (in arbitrary unit scale) were as follows:  $C_3S$  at  $32.1^\circ$ ,  $C_3A$  at  $33.1^\circ$ , CH at  $18.1^\circ$ , ettringite at  $9.0^\circ$ , ferrite (brownmillerite) at  $12.1^\circ$ , bassanite (calcium sulfate hemihydrate) at  $14.7^\circ$ , gypsum at  $11.6^\circ$ , monosulfate (monosulfoaluminate; AFm) at  $9.9^\circ$ . It should be noted that peak intensities reported in this report were not obtained using an internal standard, so intensities can only be used as an approximate indication of the amount in each phase.

### 3.3.1 Cement 1

The XRD patterns of hydrated Cement paste 1 are presented in Figure 4. The XRD peak intensities of hydrated cement 1 are summarized in Table 3.

At 5 minutes there was almost no decrease in the intensities of  $C_3S$  and  $C_3A$ . Calcium sulfate hemihydrate had disappeared and gypsum had formed. This is evidence of secondary gypsum formation. Some ettringite has also formed due to early  $C_3A$  hydration.

At 160 minutes,  $C_3A$  and  $C_3S$  intensity had decreased. The intensity of ettringite was increased. The gypsum intensity decreased only slightly. At this period, there was dissolution of calcium sulfates and calcium aluminates, but no further hydration was observed. It is assumed that some  $C_3S$  has dissolved but produced no solid hydration product.

At 385 minutes, the intensities of both gypsum and  $C_3A$  were about the same.  $C_3S$  intensity decreased and CH is observed, indicating the hydration of  $C_3S$  during this time period.

At 500 minutes, CH intensity increased substantially.  $C_3S$  hydration still dominates the hydration of cement. Gypsum intensity decreased, but  $C_3A$  intensity did not change, ettringite intensity was unchanged and no AFm was observed.

At 580 minutes, further hydration of calcium silicate was observed. There is some decrease of intensity in  $C_3A$ , gypsum was completely disappeared, but there is no significant evidence of ettringite formation or AFm formation occurring during this period.

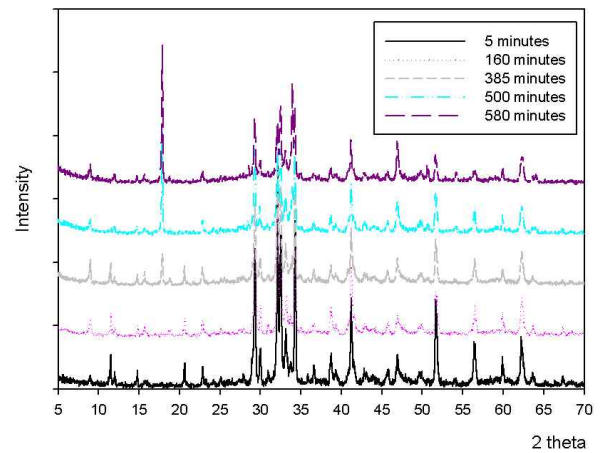


Figure 4. XRD patterns of hydrated cement 1

Table 3. XRD peak intensities (a.u.) of phases in hydrated cement 1

Time (min)	Unhydrated	5	160	385	500	580
$C_3S$	1537	1541	1261	911	791	518
$C_3A$	457	415	346	353	344	290
CH	0	0	0	278	825	1117
Ettringite	0	96	164	227	144	174
Ferrite	134	122	92	92	86	97
Bassanite*	170	0	0	0	0	0
Gypsum	83	240	202	200	71	0
Monosulfate	0	0	0	0	0	0

\*Bassanite is the mineral name of calcium sulfate hemihydrate.

### 3.3.2 Cement 2

The XRD patterns of hydrated Cement paste 2 are presented in Figure 5. Peak intensities are presented

in Table 4. The ferrite intensity in the unhydrated Cement 2 (74) is about 50% of the intensities in Cement 1 (134) and in Cement 3 (112). The color of Cement 2 is lighter than those of Cements 1 and 3.

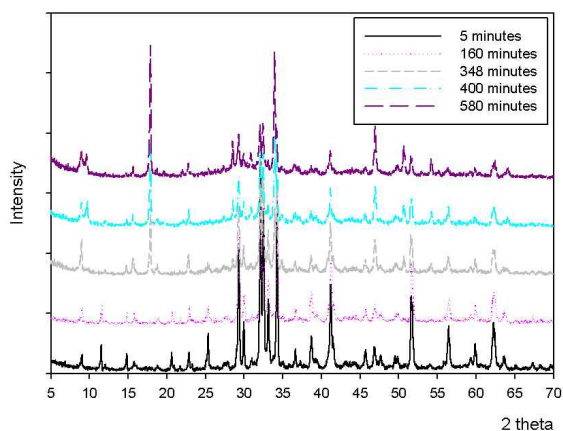


Figure 5. XRD patterns of hydrated cement 2

Table 4. XRD peak intensities (a.u.) of phases in hydrated cement 2

Time (min)	Unhydrated	5	160	348	400	580
C <sub>3</sub> S	1842	1771	1061	773	728	472
C <sub>3</sub> A	620	610	389	395	198	179
CH	0	0	0	591	734	1136
Ettringite	0	156	156	318	230	249
Ferrite	74	78	54	48	0	0
Bassanite	138	0	0	0	0	0
Gypsum	93	240	178	48	0	0
AFm	0	0	0	77	239	228

At 5 minutes, almost no decrease in the intensities of C<sub>3</sub>S and C<sub>3</sub>A was observed. Gypsum intensity increased, and calcium sulfate hemihydrate disappeared. Ettringite was formed. This is also evidence of secondary gypsum formation.

At 160 minutes, C<sub>3</sub>A and C<sub>3</sub>S intensities were decreased. No CH was observed. The intensity of ettringite was very similar to that observed at 5 min. The intensity of gypsum was decreased.

At 385 minutes, gypsum was still observed but its

intensity was further decreased. The intensity of ettringite was increased. In addition, AFm peaks were observed. High amounts of CH were observed. In this period, C<sub>3</sub>S hydration appeared to be the main reaction, with C<sub>3</sub>A hydration at the same time.

At 400 minutes, C<sub>3</sub>S intensity was almost the same, but C<sub>3</sub>A intensity was decreased. The intensity of ettringite was decreased. The intensity of AFm increased. CH was also increased. Gypsum had completely disappeared at this time. In this period, AFm formation appeared to be the main reaction, with C<sub>3</sub>S hydration at the same time.

At 580 minutes, CH intensity further increased and C<sub>3</sub>S intensity further decreased. The intensity of C<sub>3</sub>A, ettringite, and AFm were the same as for the 400 minutes sample. In this period, calcium silicate hydration appeared to be the main reaction.

### 3.3.3 Cement 3

The XRD patterns of hydrated Cement paste 3 are presented in Figure 6. Peak intensities are presented in Table 5.

At 5 minutes, calcium sulfate hemihydrate disappeared. The intensity of gypsum increased. There was a decrease in the intensities of C<sub>3</sub>S and C<sub>3</sub>A.

At 280 minutes, the intensities of C<sub>3</sub>S and C<sub>3</sub>A decreased, and the intensity of ettringite was almost the same. CH was observed. In this period, C<sub>3</sub>S and C<sub>3</sub>A reaction occurred together.

At 530 minutes, intensities of C<sub>3</sub>S and C<sub>3</sub>A further decreased. CH intensity increased substantially. All the gypsum is gone. The ettringite intensity was almost the same. However, no AFm was observed. In this period, C<sub>3</sub>S hydration appeared to be the main reaction, with some C<sub>3</sub>A hydration.

At 720 minutes, intensity of C<sub>3</sub>A further decreased. Intensity of ettringite decreased a bit. AFm was observed. It appears that AFm was mostly formed by direct reaction between C<sub>3</sub>A and gypsum, not by

conversion of ettringite. The intensity of  $C_3S$  decreased, and the intensity of CH increased. In this period,  $C_3S$  hydration and  $C_3A$  hydration occurred together.

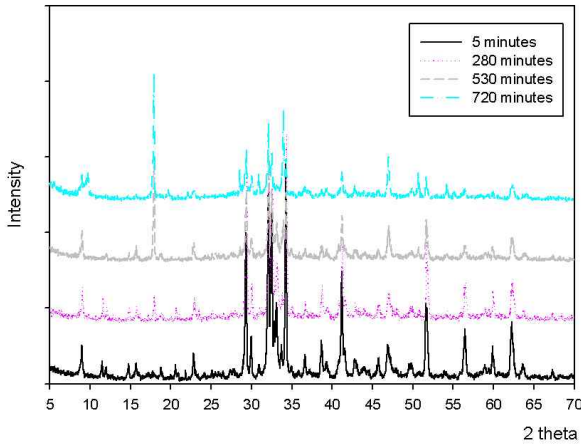


Figure 6. XRD patterns of hydrated cement 3

Table 5. XRD peak intensities (a.u.) of phases in hydrated cement 3

Time (min)	Unhydrated	5	280	530	720
$C_3S$	1621	1276	1094	718	525
$C_3A$	554	535	408	266	116
CH	0	0	161	711	845
Ettringite	0	253	241	215	181
Ferrite	112	111	92	65	59
Bassanite	142	0	0	0	0
Gypsum	62	152	161	0	0
Afm	0	0	0	0	195

### 3.4 Summary

In order to present the results more efficiently, the calorimetry curves with the hydration reactions are presented in Figures 7, 8, and 9. According to Figure 7, when Cement 1 was in contact with water, it forms secondary gypsum and ettringite. There was some time period without any significant reaction (noted by a decrease in  $dT/dt$  curve), and the hydration of  $C_3S$  and  $C_3A$  resumed. The peak of the curve was due to the hydration of  $C_3S$ , and the shoulder peak after about 500 minutes was associated with  $C_3S$  and

$C_3A$  (continuous formation of ettringite).

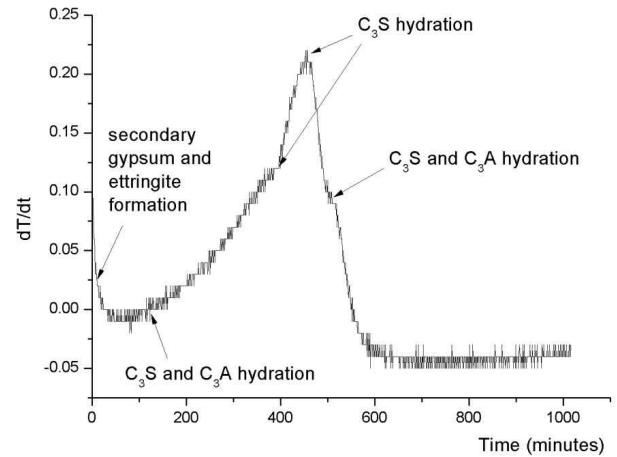


Figure 7. Hydration reaction of cement 1

It was found that Cement 2 also showed secondary gypsum and ettringite formation at 5 minutes. There was also some time period without any significant reaction (noted by decrease in  $dT/dt$  curve) followed by hydration of  $C_3S$  and  $C_3A$ . Differently from Cement 1, the peak of the curve was associated with the hydration of  $C_3S$  and  $C_3A$  (formation of AFm). In addition, compared to Cement 1, the  $C_3A$  in this cement hydrated faster.

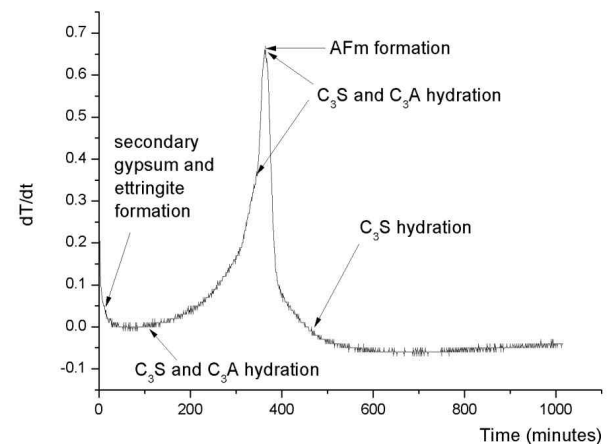


Figure 8. Hydration reaction of Cement 2

Cement 3 also showed secondary gypsum and ettringite formation at 5 minutes. Hydration of  $C_3S$



and  $C_3A$  followed after. Unlike Cement 1 and Cement 2, two peaks were identified in  $dT/dt$  curve. The first peak was associated with the hydration of  $C_3S$  and  $C_3A$  (formation of ettringite). The second peak was also associated with the hydration of  $C_3S$  and  $C_3A$ , but in this case, hydration of  $C_3A$  is to form AFm.

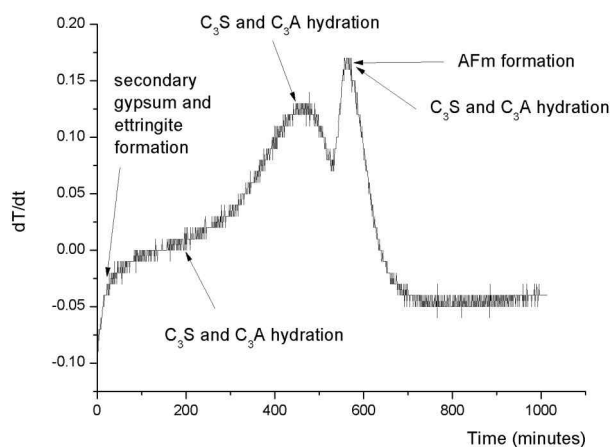


Figure 9. Hydration reaction of cement 3

## 4. Conclusions

Based on the results provided in this work, the following conclusions can be drawn.

- 1) All cement showed secondary gypsum formation.
- 2) The approach of using first derivative of temperature rise ( $dT/dt$ ) curve to isolate individual peaks related to the hydration of cement phases was successful.
- 3) Using  $dT/dt$  curve with XRD, hydration characteristics of cement can be investigated.

## Acknowledgement

This work was supported by a Research Grant of Pukyong National University (2014Year). (C-D-2014-0487)

## References

1. Laidler KJ, Gerischer H. The world of physical chemistry, Vol. 3, United Kingdom:Oxford University Press;1995, 476p.
2. Bensted J. Some applications of conduction calorimetry 10 cement hydration. *Advances in Cement Research*, 1987 Oct;1(1):35-44.
3. Taplin JM. A method for following the hydration reaction in Portland cement paste. *Australian Journal of Applied Science*, 1959;10(3):329-45.
4. Young JF. Hydration of Portland cement. In: *Instructional modulus in cement science*, ed. D. M. Roy. USA: Materials education Council, Materials Research Laboratory, University Park, PA;1985, 1087p.
5. Bailyn M. *A Survey of Thermodynamics*. American, New York: Institute of Physics Press;1994, 791 p.
6. Bentz DP, Waller V, De Larrard F. Prediction of adiabatic temperature rise in conventional and high-performance concretes using a 3-D microstructural model. *Cement and Concrete Research*, 1998 Feb;28(2):285-297.
7. Yiwang Bao, Li Tian, Jianghong Gong. Testing Methods of Adiabatic Temperature Rise in Concrete. *Advanced Materials Research*, 2011 Mar;177:574-77.
8. Abdol R, Chini and Arash Parham. Adiabatic temperature rise of mass concrete in Florida, Florida: Report Submitted to Florida Department of Transportation(USA); 2005. Report No.:Final report.
9. Christensen BJ. Significance of Tests and Properties of Concrete and Concrete-Making Materials, ASTM STP 169D. Philadelphia(USA): Lamond JF and Pielert JH; 2006 April, Chapter 11, Time of setting; p.86-98.
10. Sandberg JP, Liberman S. Monitoring and Evaluation of Cement Hydration by Semi-Adiabatic Field Calorimetry. *ACI Special Publication*, 2007;241:13-24.
11. ASTM C150, Standard Specification for Portland Cement, Annual Book of ASTM Standards, Vol. 04, 01, ASTM International, West Conshohocken, PA, 2008.
12. ASTM C305, Standard Practice for Mechanical Mixing of Hydraulic Cement Pastes and Mortars of Plastic Consistency, Annual Book of ASTM Standards, Vol. 04,01, ASTM International, West Conshohocken, PA, 2006.